Low-Temperature Nanoparticle-Directed Solid-State Synthesis of Ternary and Quaternary Transition Metal Oxides

Amanda E. Henkes, J. Chris Bauer, Amandeep K. Sra, Raiman D. Johnson, Robert E. Cable, and Raymond E. Schaak*

Department of Chemistry, Texas A&M University, College Station, Texas 77842-3012

Received September 30, 2005. Revised Manuscript Received October 27, 2005

Ternary and quaternary transition metal oxides, which offer a wide variety of important physical properties, are traditionally synthesized using high-temperature reactions that often require several days of heating. A new nanoparticle-directed approach for the rapid low-temperature synthesis of nanocrystalline bulk-scale ternary and quaternary transition metal oxides has been developed. Readily available metal oxide nanoparticles can serve as a robust toolkit of highly reactive reagents, which can be mixed in solution in known ratios to form nanomodulated precursors and rapidly transformed, at relatively low temperatures, into more complex oxides. This approach is initially demonstrated for pyrochlore-type $Y_2Ti_2O_7$ and $Eu_2Ti_2O_7$ using XRD, DSC, and TEM to monitor the reaction. A nanocomposite of Y_2O_3 and TiO_2 nanoparticles transforms into nanocrystalline $Y_2Ti_2O_7$ within 2 h of heating to 700 °C, and $Eu_2Ti_2O_7$ forms within 2 h of heating a nanocomposite of Eu_2O_3 and TiO_2 nanoparticles to 800 °C. $NiTiO_3$, $CoTiO_3$, Bi_2CuO_4, and $Bi_5FeTi_3O_{15}$ can also be synthesized.

Introduction

Ternary and quaternary transition metal oxides offer a wide variety of important physical properties, including magnetism,[1] superconductivity,[2] ferroelectricity,[3] nonlinear optical behavior,[4] ionic conductivity,[5] and catalytic activity.[6] Like all solid-state materials, the synthesis of multi-metal oxides is critical for ensuring optimal performance. These oxides are traditionally synthesized using high-temperature reactions that often require several days of heating because solid−solid diffusion is the rate-limiting step in their formation. As a result, the phases that form are generally thermodynamically stable, and there is little control over the morphology or the kinetics of phase formation. Alternative methods exist for synthesizing metal oxides at low temperatures, including coprecipitation,[7] hydrothermal synthesis,[8] topochemical reactions,[9] and the sol−gel process,[10] and they are generally successful at yielding simple oxides with some control over structure, morphology, and processability. Each of these alternative low-temperature synthetic methods has a particular strength, and often the synthesis of new functional materials is driven by their use.

Here, we present a new nanoparticle-directed approach for the rapid low-temperature synthesis of bulk-scale ternary and quaternary transition metal oxides. Our strategy is based on the idea that readily available binary oxide nanoparticles can serve as a robust toolkit of reactants that can be combined in known ratios to form nanocomposites and then thermally transformed rapidly and at low temperatures into a predesigned product phase. Since solid−solid diffusion is the rate-limiting step in traditional solid-state reactions, this alternative approach succeeds because it effectively reduces diffusion distances to the nanometer scale and allows reactions to occur much more quickly at relatively low temperatures. This synthetic strategy employs much milder conditions than are required for traditional approaches, including water-based mixing of the solid-state precursors and heating temperatures that are often 400−700 °C lower than necessary for conventional high-temperature routes. This approach was originally developed for the low-temperature solution-based synthesis of alloys and intermetallic compounds[11,12] and has yielded insights into reaction pathways and has the potential to generate new structures that are not stable in bulk systems synthesized through traditional methods. Extending this approach to oxides is important because it opens the door to studying low-temperature phase formation and kinetically controlling reaction pathways for these materials. Furthermore, because of the availability of many metal oxide nanoparticles that can serve as precursors,[13]

* To whom correspondence should be addressed: Department of Chemistry, Texas A&M University, P.O. Box 30012, College Station, TX 77842-3012. E-mail: schaak@mail.chem.tamu.edu. Phone: (979)458-2858. Fax: (979)845-4719.

(1) Salamon, M. B.; Jaime, M. *Rev. Mod. Phys.* **2001**, *73*, 583−628.
(2) Cava, R. J. *J. Am. Ceram. Soc.* **2000**, *83*, 5−28.
(3) Nanamatsum S.; Kimura, M.; Doi, K.; Matsushita, S.; Yamada, N. *Ferroelectrics* **1974**, *8*, 511−513.
(4) Halasyamani, P. S.; Poeppelmeier, K. R. *Chem. Mater.* **1998**, *10*, 2753−2769.
(5) Boivin, J. C.; Mairesse, G. *Chem. Mater.* **1998**, *10*, 2870−2888.
(6) Pena, M. A.; Fierro, J. L. G. *Chem. Rev.* **2001**, *101*, 1981−2017.
(7) Rao, C. N. R.; Gopalakrishnan, J. *New Directions in Solid State Chemistry*; Cambridge University Press: Cambridge, 1989.
(8) Feng, S.; Xu, R. *Acc. Chem. Res.* **2001**, *34*, 239.
(9) (a) Schaak, R. E.; Mallouk, T. E. *J. Am. Chem. Soc.* **2000**, *122*, 2798−2803. (b) Schaak, R. E.; Mallouk, T. E. *Chem. Mater.* **2002**, *14*, 1455−1471.
(10) Wright, J. D.; Sommerdijk, A. J. M. *Sol−gel materials: chemistry and applications*; Gordon and Breach: Amsterdam, 2001.
(11) Sra, A. K.; Schaak, R. E. *J. Am. Chem. Soc.* **2004**, *126*, 6667−6672.
(12) Schaak, R. E.; Sra, A. K.; Leonard, B. M.; Cable, R. E.; Bauer, J. C.; Han, Y.-F.; Means, J.; Teizer, W.; Vasquez, Y.; Funck, E. S. *J. Am. Chem. Soc.* **2005**, *127*, 3506−3515.
(13) Cushing, B. L.; Kolesnichenko, V. L.; O'Connor, C. J. *Chem. Rev.* **2004**, *104*, 3893−3946.

10.1021/cm052190o CCC: $33.50
Published on Web 12/14/2005

this approach has the potential to be general for a wide range of complex systems. As an alternative to other approaches for forming mixed-metal oxides, this strategy may offer different types of control over particle size, morphology, and materials processing capabilities, as well as the ability to access multi-metal oxides at low temperatures without the need for first generating complex molecular precursors or utilizing reaction conditions that are highly sensitive to pH, chemical environment, or elemental composition and stoichiometry.

Experimental Section

Synthesis of Nanoparticle Precursors (Y_2O_3, Eu_2O_3, TiO_2, NiO, Cu_2O, Bi_2O_3, Fe_2O_3). To synthesize nanoparticles of Y_2O_3, Eu_2O_3, NiO, CoO, and Cu_2O, the appropriate metal salts were dissolved in 15 mL of NANOpure water (18.2 MΩ) along with 100 mg of poly(vinyl pyrrolidone) (PVP, MW = 40000). The metal salts and their amounts were $Y(C_2H_3O_2)_3{\cdot}4H_2O$ (24.0 mg, 0.0710 mmol), $Eu(NO_3)_3{\cdot}6H_2O$ (34.0 mg, 0.0762 mmol), $Ni(C_2H_3O_2)_2{\cdot}xH_2O$ (21.5 mg, 0.08166 mmol, accounting for the exact number of waters of hydration determined by TGA analysis in air), $CoCl_2{\cdot}6H_2O$ (18.9 mg, 0.0794 mmol), $Cu(C_2H_3O_2)_2{\cdot}H_2O$ (19.0 mg, 0.0952 mmol), and $FeCl_3{\cdot}6H_2O$ (20.3 mg, 0.0751 mmol). $NaBH_4$ (10 mg, 0.2645 mmol) was then added to the metal salt solutions with stirring to initially form reduced metal nanoparticles, and stirring was allowed to continue for 30−60 min in air to oxidize the particles (CoO required 3−4 h of stirring). (For Y^{3+} and Eu^{3+}, which are not reducible by $NaBH_4$, this process facilitated precipitation of the oxide without reduction.) The solutions were centrifuged at 13000 rpm, and the precipitated oxides were washed several times with ethanol and dried under ambient conditions. To synthesize TiO_2 nanoparticles, titanium isopropoxide (2.0 mL, 0.0351 M in 2-propanol) was added dropwise to 20 mL of H_2O and 100 mg of PVP to initiate the hydrolysis reaction, forming TiO_2. The solution was stirred for 15−30 min and then centrifuged at 13000 rpm. To synthesize Bi_2O_3 nanoparticles (based on ref 14), $Bi(NO_3)_3{\cdot}5H_2O$ (1.66 g) was dissolved in 50 mL of diethylene glycol with sonication. NaOH (1 mL, 0.1 M) was then added, and the solution was heated to 140 °C for 1 h prior to raising the temperature to 180 °C for 2 h. The solution was then cooled to room temperature, and the Bi_2O_3 nanoparticles were isolated by centrifugation at 13000 rpm. The precipitated oxides were washed several times with ethanol and dried under ambient conditions.

Formation of Nanocomposites and Conversion into Oxide Products. $Y_2Ti_2O_7$ was formed using two procedures. First, approximately 5.6 mg of Y_2O_3 and approximately 8.0 mg of TiO_2 nanoparticle powders (as-synthesized in solution) were re-dispersed in 40 mL of H_2O and stirred for 30 min, and the precipitate (Y_2O_3:TiO_2 nanocomposite) was isolated by centrifugation. In a slight modification of this procedure, Y_2O_3:TiO_2 nanocomposites could also be accessed by adding titanium isopropoxide (2.0 mL, 0.0351 M in 2-propanol) to the as-synthesized Y_2O_3 nanoparticle solution, essentially forming TiO_2 nanoparticles in situ in the presence of Y_2O_3 nanoparticles. TEM analysis confirmed the presence of a Y_2O_3:TiO_2 nanoparticle composite identical to the one formed by physically mixing Y_2O_3 and TiO_2 nanoparticles. In both cases, the nanocomposite was heated in air to temperatures between 500 and 1000 °C for time intervals of 30 min to 6 h. Optimal heating time for accessing pyrochlore-type $Y_2Ti_2O_7$ was 700 °C for 2 h. Both synthetic approaches yielded $Y_2Ti_2O_7$. The other phases were synthesized in an identical manner to $Y_2Ti_2O_7$ (both methods), using different nanoparticles as precursors: $Eu_2Ti_2O_7$ (800 °C, 2 h), $NiTiO_3$ (700 °C, 1 h), $CoTiO_3$ (700 °C, 2 h), Bi_2CuO_4 (500 °C, 2 h), and $Bi_5FeTi_3O_{15}$ (700 °C, 2 h). Note that, for the Bi_2CuO_4 system, the Cu_2O nanoparticles oxidize to CuO upon heating, so the metal salt ratios were based on the final CuO product that is stable at the final heating temperature. XRD patterns for the nanoparticle precursors, both as-synthesized and after heating to 500 °C, are shown in the Supporting Information.

Characterization Details. Powder X-ray diffraction (XRD) data were collected using a Bruker GADDS three-circle X-ray diffractometer (Cu Kα radiation, 40 mV, 40 mA) using microdiffraction powder techniques.[15] The large background at low angles is due to air scattering because the beam size is larger than the sample for the microdiffraction experiments.[15] Transmission electron microscopy (TEM) images, energy-dispersive X-ray spectroscopy (EDS), and selected area diffraction (SAED) patterns were collected on a JEOL 2010 TEM operating at 200 kV. Samples were prepared by re-suspending the isolated and cleaned nanoparticles in ethanol and dropping the solution on a carbon-coated Cu or Ni grid (chosen to avoid EDS interference with constituent elements in the samples). Differential scanning calorimetry (DSC) data were collected on a TA Instruments Q600 SDT under flowing air at a heating rate of 10 °C/min. Elemental analysis for C, H, and N (CHN analysis) was performed by Atlantic Microlabs (Norcross, GA).

Results and Discussion

As an initial demonstration of the applicability of the nanoparticle precursor route to multi-metal oxides, we focused on pyrochlore-type $Y_2Ti_2O_7$. Titanate pyrochlores are important oxides with properties that include geometric magnetic frustration[16] and high-T_c ferroelectricity,[3] and $Y_2Ti_2O_7$ in particular shows ionic conductivity when appropriately doped.[17] $Y_2Ti_2O_7$ is traditionally synthesized by heating mechanically mixed powders of Y_2O_3 and TiO_2 to temperatures above 1200 °C for 1−3 days.[18] Alternative methods for synthesizing $Y_2Ti_2O_7$[19−21] have yielded products that either contain significant amounts of organic residue, are limited to thin films, or require long reaction times to yield a phase-pure product. With use of our nanoparticle-directed strategy, bulk-scale $Y_2Ti_2O_7$ can be formed within 2 h of heating at 700 °C.

Figure 1a shows powder XRD data for Y_2O_3 and TiO_2 nanoparticles stabilized by poly(vinyl pyrrolidone) (PVP) that were synthesized using standard solution techniques. The Y_2O_3 and TiO_2 nanoparticles appear to be amorphous as synthesized at room tempertaure, but upon annealing them to 500 °C, they crystallize to form phase-pure cubic Y_2O_3

(14) Feldmann, C. *J. Mater. Res.* **2000**, *15*, 2244−2248.

(15) (a) Bhuvanesh, N. S. P.; Reibenspies, J. H. *J. Appl. Crystallogr.* **2003**, *36*, 1480−1481. (b) Bhuvanesh, N. S. P.; Reibenspies, J. H.; Zhang, Y.; Lee, P. L. *J. Appl. Crystallogr.* **2005**, *38*, 632−638.

(16) Snyder, J.; Slusky, J. S.; Cava, R. J.; Schiffer, P. *Nature* **2001**, *413*, 48−51.

(17) Heremans, C.; Wuensch, B. J.; Stalick, J. K.; Prince, E. *J. Solid State Chem.* **1995**, *117*, 108−121.

(18) (a) Wang, S. X.; Wang, L. M.; Ewing, R. C.; Govindan Kutty, K. V. *Nucl. Instrum. Methods B* **2000**, *169*, 135−140. (b) Hayward, M. A. *Chem. Mater.* **2005**, *17*, 670−675.

(19) Fuentes, A. F.; Boulahya, K.; Maczka, M.; Hanuza, J.; Amador, U. *Solid State Sci.* **2005**, *7*, 343−353.

(20) Kakihana, M.; Milanova, M. M.; Arima, M.; Okubo, T.; Yashima, M.; Yoshimura, M. *J. Am. Ceram. Soc.* **1996**, *79*, 1673−1676.

(21) (a) Langlet, M.; Jenouvrier, P.; Rimet, R.; Fick, J. *Opt. Mater.* **2004**, *25*, 141−147. (b) Jenouvrier, P.; Boccardi, G.; Fick, J.; Jurdyc, A.-M.; Langlet, M. *J. Lumin.* **2005**, *113*, 291−300.

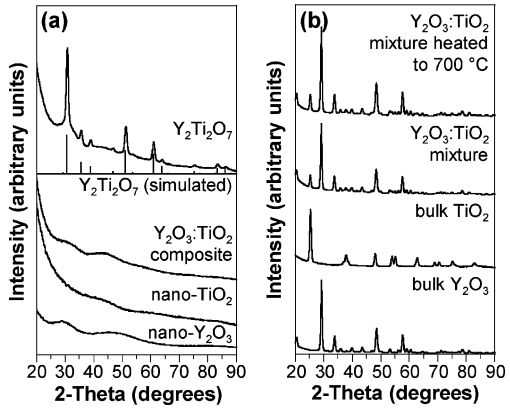

Figure 1. (a) Powder XRD patterns for Y_2O_3 and TiO_2 nanoparticles, a 1:2 Y_2O_3:TiO_2 nanocomposite, and the nanocomposite heated to 700 °C for 2 h to form pyrochlore-type $Y_2Ti_2O_7$ (top XRD pattern). The simulated XRD pattern for $Y_2Ti_2O_7$, based on PDF card #42-0413, is shown for comparison. (b) For comparison, analogous XRD data for bulk-scale (micrometer-size) samples of Y_2O_3, TiO_2, a mechanically mixed Y_2O_3−TiO_2 sample, and the 1:2 Y_2O_3:TiO_2 mixture heated to 700 °C for 4 h. No appreciable reaction is observed under similar heating conditions to those used in (1).

and anatase TiO_2, as expected (see Supporting Information). When re-dispersed in water in a 1:1 molar ratio of Y_2O_3:TiO_2, a nanocomposite forms and precipitates out of solution. The initial mass is not all recovered, indicating that the nanocomposite formation is not quantitative, although, in most cases, the nominal ratio of nanoparticles mixed together agrees well with the actual composition of the precipitated nanocomposite (quantitative data for each system are given in the text that follows). In most cases, the individual nanoparticles will precipitate out of solution over time, regardless of whether they have been mixed with other types of nanoparticles. We speculate that the solution mixing, combined with known interactions of polymers in solution, homogenizes the nanoparticles, effectively mixing them at the 10−100 nm scale and allowing them to coprecipitate in a reasonably homogeneous fashion. The precipitated nanocomposite was found by EDS analysis to have an average Y:Ti stoichiometry of 1.1:1.0, which is close to that of the relative ratios of the Y_2O_3 and TiO_2 nanoparticles in solution. In addition, TGA analysis in air indicates that the nanocomposite contains 25−30 wt % PVP. The XRD pattern (Figure 1a) for the Y_2O_3:TiO_2 nanocomposite has broad peaks that generally match those expected for a mixture of amorphous Y_2O_3 and TiO_2.

Figure 2 shows transmission electron microscopy (TEM) images of the nanoparticles and nanocomposite. The Y_2O_3 system (Figure 2a) appears as a network of irregularly shaped nanoparticles with diameters that range from 5 to 15 nm. The selected-area electron diffraction (SAED) pattern (Figure 2a, inset) is very diffuse, which is consistent with the broad XRD pattern and indicates an amorphous structure. The TiO_2 nanoparticles, shown in Figure 2b, generally form larger 20−50 nm blocks which, upon closer inspection, are comprised of 1−3 nm particles. The SAED pattern is almost featureless, also indicating an amorphous structure. The Y_2O_3:TiO_2 nanocomposite (Figure 2c) formed in solution from the aggregation of the PVP-stabilized Y_2O_3 and TiO_2 nanoparticles shows a mixture of the interconnected Y_2O_3 nanoparticles and the spongelike TiO_2 nanoparticles (enlarged

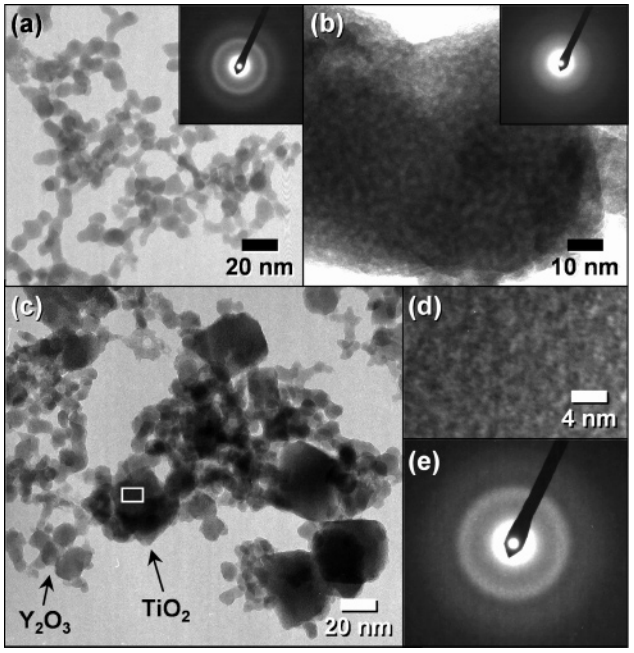

Figure 2. TEM micrographs of (a) Y_2O_3 nanoparticles, (b) TiO_2 nanoparticles, and (c) the Y_2O_3:TiO_2 nanocomposite showing components consistent with both Y_2O_3 and TiO_2. An enlargement of the region marked by a box in (c) is shown in (d), and it matches the spongelike structure observed for TiO_2 nanoparticles. SAED patterns for the Y_2O_3 and TiO_2 nanoparticles are shown as insets in (a) and (b), and the SAED pattern for the nanocomposite is shown in (e).

view of the TiO_2 region is shown in Figure 2d). EDS confirms the presence of both Ti and Y in a 1.0:1.1 ratio, and the SAED pattern (Figure 2e) shows primarily the diffraction pattern expected for Y_2O_3, with extra diffuse intensity like that observed for TiO_2.

When the nanocomposite is heated to 700 °C for 2 h in air, the resulting XRD pattern (Figure 1a) matches that expected for pyrochlore-type $Y_2Ti_2O_7$ (PDF card #42-0413). The resulting powder (Figure 3) is nanocrystalline, with 50−100 nm grains. Importantly, elemental analysis for carbon, hydrogen, and nitrogen indicates that 100% of the polymer residue is removed (via oxidation) during the heating process, leaving a product that is free of organic impurities.

In contrast to the nanoparticle-directed synthesis of $Y_2Ti_2O_7$, which yields a crystalline pyrochlore phase at temperatures as low as 700 °C, the traditional high-temperature ceramic method is virtually unreactive at these temperatures. Figure 1b shows powder XRD data for micrometer-scale Y_2O_3 and TiO_2 powders, as well as the 1:1 physical mixture of Y_2O_3 and TiO_2. When the mixture of micrometer-scale Y_2O_3 and TiO_2 powders are heated to 700 °C for several hours, no reaction is detected (Figure 1b). This clearly shows the enhanced reactivity afforded by the nanoparticle precursors, which decrease diffusion distances by several orders of magnitude and virtually eliminate solid−solid diffusion as the rate-limiting step.

Similarly, phase-pure pyrochlore-type $Eu_2Ti_2O_7$ can be prepared by heating a composite of Eu_2O_3 and TiO_2 nanoparticles (1.0:1.1 average Eu:Ti stiochiometry according to EDS analysis) to 800 °C for 2 h (Figure 4a). Interestingly, the differential scanning calorimetry (DSC) trace for the Eu_2O_3:TiO_2 nanocomposite (Figure 4b) shows an exotherm

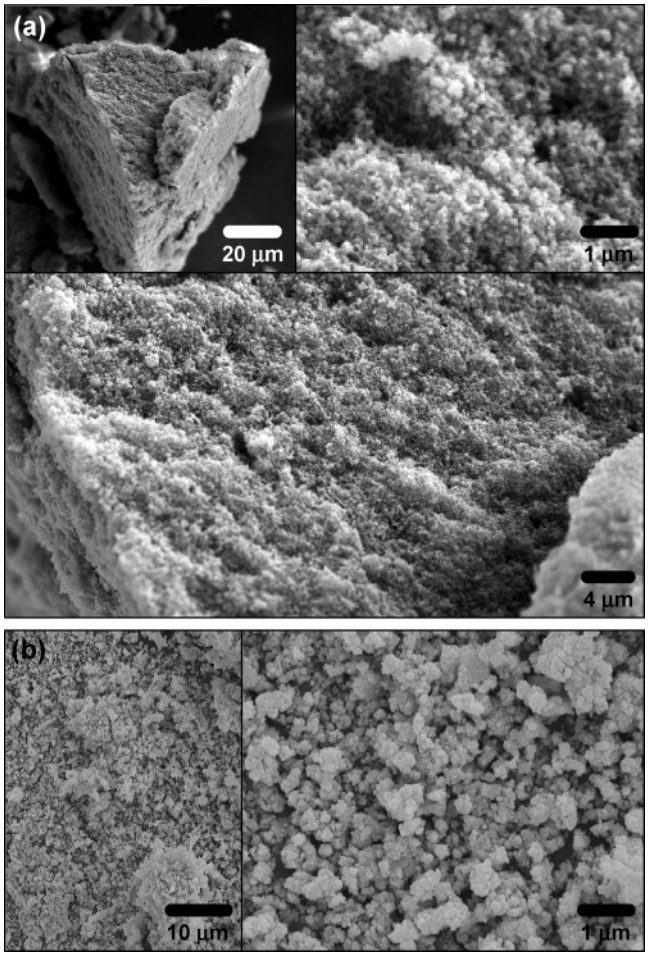

Figure 3. (a) SEM micrographs (three magnifications of the same sample) for nanocrystalline pyrochlore-type $Y_2Ti_2O_7$ powder prepared by heating a 1:2 Y_2O_3:TiO_2 nanocomposite to 700 °C for 2 h and (b) SEM micrographs of nanocrystalline Bi_2CuO_4 powder synthesized from nanoparticles of Bi_2O_3 and Cu_2O (oxidized in situ to CuO).

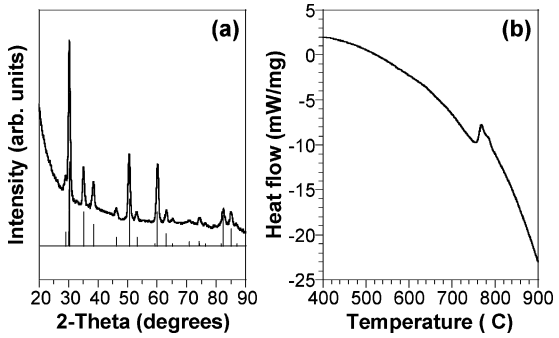

Figure 4. (a) XRD pattern for the pyrochlore-type $Eu_2Ti_2O_7$ product formed by heating a Eu_2O_3:TiO_2 nanocomposite to 800 °C for 1 h. The simulated XRD pattern is shown for comparison. (b) DSC trace (in air) for a 1:2 Eu_2O_3:TiO_2 nanocomposite, showing an exotherm near 765 °C that corresponds to the crystallization of pyrochlore-type $Eu_2Ti_2O_7$.

at 765 °C. (The Y_2O_3:TiO_2 nanocomposite shows similar features.) Previous calorimetry studies of ball-milled $RE_2Ti_2O_7$ (RE = rare earth) attribute this exotherm to atomic ordering that forms the pyrochlore lattice.[19] For traditional bulk powders, this feature is not observed because diffusion is not complete on the time scale of the calorimetry experiment. However, RE_2O_3:TiO_2 powders that are broken into smaller pieces and homogenized by extensive mechanical milling show similar exotherms.[19] Thus, observation of this exotherm in our samples is further evidence of solution-mediated nanocomposite formation and its role in supporting rapid thermal interdiffusion of the reagents to nucleate $Eu_2Ti_2O_7$ and $Y_2Ti_2O_7$.

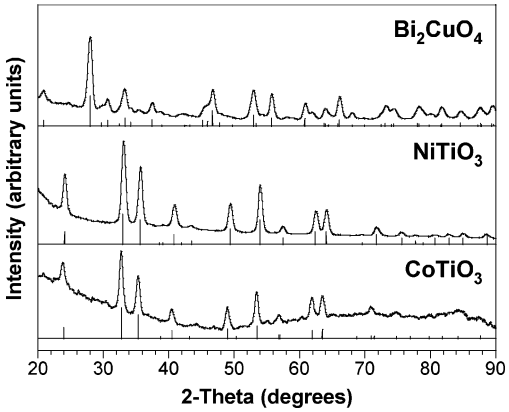

Figure 5. Powder XRD patterns and simulated XRD data for $CoTiO_3$ (CoO:TiO_2 nanoparticle composite, 700 °C, 2 h), $NiTiO_3$ (NiO:TiO_2 nanoparticle composite, 700 °C, 1 h), and Bi_2CuO_4 (Bi_2O_3:CuO nanoparticle composite, 500 °C, 2 h).

In addition to $Y_2Ti_2O_7$ and $Eu_2Ti_2O_7$, other ternary oxides can be accessed using this method. For example, Figure 5 shows the XRD pattern for ilmenite-type $NiTiO_3$ that was synthesized from a composite containing nanoparticles of NiO and TiO_2. $NiTiO_3$ is typically synthesized at 1000−1400 °C,[22] and while a few lower temperature methods have been reported,[23] they generally contain significant amounts of impurities. Here, we accessed phase-pure $NiTiO_3$ by heating a NiO:TiO_2 nanocomposite to 700 °C for 1 h. Ilmenite-type $CoTiO_3$ can also be synthesized by heating a CoO:TiO_2 nanocomposite (1.0:1.1 ratio of Co:Ti according to EDS analysis) to 700 °C for 2 h. Likewise, Bi_2CuO_4 can be formed as low as 500 °C (2 h) from a composite of Cu_2O and Bi_2O_3 nanoparticles. (Recall that the Cu_2O nanoparticles oxidize to CuO when heated to 500 °C.) The powders also remain nanocrystalline (Figure 3b), as observed for $Y_2Ti_2O_7$ using the same synthetic strategy. It appears that this approach is general for a variety of ternary oxide systems.

Furthermore, by forming a nanocomposite of Bi_2O_3, Fe_2O_3, and TiO_2 nanoparticles mediated by solution-phase mixing, the quaternary oxide $Bi_5FeTi_3O_{15}$[24] can be formed. Aurivillius-type $Bi_5FeTi_3O_{15}$, which is both ferroelectric and antiferromagnetic,[24] forms upon heating the three-component nanocomposite to 700 °C for 2h (Figure 6). The three-component nanocomposite was found to have Bi:Fe:Ti ratios of 3.3:1.0:1.8 according to EDS analysis, which corresponds to an average composition of $Bi_{5.5}Fe_{1.7}Ti_{3.0}O_{15}$ when normalized to Ti. Considering the inherent error in the EDS analysis, this agrees reasonably well with the expected stoichiometry, although it may suggest that some excess Bi_2O_3 and Fe_2O_3 remains amorphous and unreacted or incorporates as inter-

(22) Lerch, M.; Boysen, H.; Neder, R.; Frey, F.; Laqua, W. *J. Phys. Chem. Solids* **1992**, *53*, 1153−1156.
(23) Taylor, D. J.; Fleig, P. F.; Page, R. A. *Thin Solid Films* **2002**, *408*, 104−110.
(24) (a) Singh, R. S.; Bhimasankaram, T.; Kumar, G. S.; Suryanarayana, S. V. *Solid State Commun.* **1994**, *91*, 567−569. (b) Srinivas, A.; Suryanarayana, S. V.; Kumar, G. S.; Kumar, M. M. *J. Phys. Condens. Matter* **1999**, *11*, 3335−3340. (c) Srinivas, A.; Kim, D.-W.; Hong, K. S.; Suryanarayana, S. V. *Mater. Res. Bull.* **2004**, *39*, 55−61.

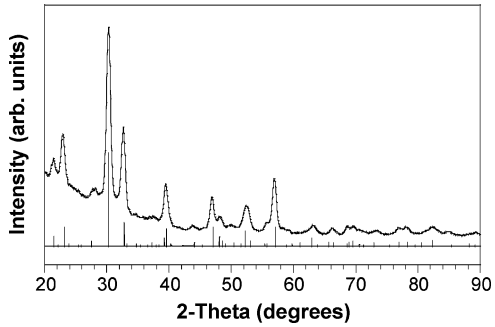

Figure 6. Powder XRD pattern and simulated XRD data for Aurivillius-type $Bi_5FeTi_3O_{15}$ synthesized by heating a Bi_2O_3:Fe_2O_3:TiO_2 nanocomposite to 700 °C for 2 h.

growths in the layered structure, or that some of the TiO_2 remains in solution and does not precipitate. Regardless, the low-temperature formation of Aurivillius-type $Bi_5FeTi_3O_{15}$ is in contrast to the traditional synthesis of this phase, which requires heating to 1050 °C.[24] Thus, in addition to ternary oxides, quaternary oxides can be formed using this method. This suggests that a variety of compositionally and structurally complex oxides could be formed as nanocrystalline powders at low temperatures using this strategy.

Conclusions

In summary, we have shown that readily available metal oxide nanoparticles can serve as a robust toolkit of highly reactive reagents, which can be mixed in solution in known ratios to form nanomodulated precursors that rapidly transform, at low temperatures and under mild conditions, into complex ternary and quaternary oxides. This represents a new low-temperature approach for synthesizing nanocrystalline oxides that is distinct from other methods. In all cases, this approach can nucleate complex crystalline oxides at temperatures that are equal to or lower than the crystallization temperatures observed using other methods. While most of our target compounds can be prepared by other methods such as coprecipitation, the use of nanoparticles as precursors opens up new possibilities for solution-based materials processing applications, control of nanocrystalline morphology, and careful studies of diffusion and nucleation events in nanoscale oxide materials. Accordingly, in analogy to our previous work with alloys and intermetallic compounds,[11,12] it may prove possible to study reaction pathways, separate diffusion and nucleation events, template nanostructured materials using solution infiltration routes, and synthesize new and metastable phases in bulk-scale oxide systems using this approach. Modifications to this approach may also provide insight into the size dependence of crystallization temperatures for complex oxides, carefully tuning the composite homogeneity from nearly atomic-level mixing (e.g., coprecipitation) to the micrometer-scale mixing of traditional ceramic samples since many of the nanoparticle precursors can be made as size-controlled nanocrystals with dimensions that span several orders of magnitude.[25] Finally, this work demonstrates that the same synthetic concept can be applied to both oxides and reduced multi-metallic compounds and suggests that this strategy may be general for many other classes of solid-state materials.

Acknowledgment. This work was supported by start-up funds from Texas A&M University and funding from the Robert A. Welch Foundation (Grant No. A-1583). Acknowledgment is made to the Donors of the American Chemical Society Petroleum Research Fund for partial support of this research. Electron microscopy was performed at the Microscopy and Imaging Center at Texas A&M University.

Supporting Information Available: Powder XRD data for nanocrystalline precursors (PDF). This material is available free of charge via the Internet at http://pubs.acs.org.

CM052190O

(25) (a) Fedlmann, C.; Jungk, H.-O. *Angew. Chem., Int. Ed.* **2001**, *40*, 359−362. (b) Li, X.; Gao, H.; Murphy, C. J.; Gou, L. *Nano Lett.* **2004**, *4*, 1903−1907. (c) Stewart, S. J.; Multigner, M.; Marco, J. F.; Berry, F. J.; Hernando, A.; Gonzalez, J. M. *Solid State Commun.* **2004**, *130*, 247−251. (d) Wang, Z.; Chen, X.; Liu, J.; Mo, M.; Yang, L.; Qian, Y. *Solid State Commun.* **2004**, *130*, 585−589. (e) Yin, M.; Wu, C.-K.; Lou, Y.; Burda, C.; Koberstein, J. T.; Zhu, Y.; O'Brien, S. *J. Am. Chem. Soc.* **2005**, *127*, 9506−0511.